Rotating electro-osmotic flow over a plate or between two plates

Chien-Cheng Chang[1,2,*] and Chang-Yi Wang[1,3]

[1]*Division of Mechanics, Research Center for Applied Sciences, Academia Sinica, Taipei 115, Taiwan*

[2]*Institute of Applied Mechanics and Taida Institute of Mathematical Sciences, National Taiwan University, Taipei 106, Taiwan*

[3]*Department of Mathematics and Department of Mechanical Engineering, Michigan State University, East Lansing, Michigan 48824, USA*

(Received 8 June 2011; revised manuscript received 28 September 2011; published 22 November 2011)

In this paper, we investigate rotating electro-osmotic (EO) flow over an infinite plate or in a channel formed by two parallel plates. The analysis is based on the Debye-Hückel approximation for charge distributions and the Navier-Stokes equation for a transport electrolyte in the rotating frame. It is shown that, for the single plate, the nondimensional speed of system rotation ω is the singly most important parameter, while for the channel, in addition to ω, the nondimensional electrokinetic width K also plays an important role. However, the parameter $\omega \equiv \eta^2$ has different natural appearances in the respective cases of a single plate (SP) and two plates (TPs). More precisely, η(SP) measures the ratio λ_D/L_K of the Debye length to the Ekman depth, while η(TP) measures the ratio L/L_K of the channel width to the Ekman depth. The effect of rotation is always to reduce the axial flow rate along the direction of the applied electric field, accompanied by a (secondary) transverse flow. In the SP case, the plot on the velocity plane for each ω shows an interesting closed EO Ekman spiral. The size of the spiral shrinks with increasing ω. The transverse flow is so significant that the volume transport associated with the EO Ekman spiral turns clockwise 45° to the applied field near $\omega = 0$ and gradually turns at a right angle to the applied field as ω is increased. In contrast, in the TP case, the transverse flow rate is smaller than the axial flow rate when ω is small. The transverse flow rates at all K are observed to reach their maxima at ω of order 1. The volume transport is nearly at a zero angle to the applied field near $\omega = 0$ and gradually turns to 45° to the applied field as ω is increased. In the limit of $\omega \to \infty$, for both SP and TP cases, the entire system forms a rigid body rotation—there is neither axial nor transverse flow.

DOI: 10.1103/PhysRevE.84.056320 PACS number(s): 47.61.−k

I. INTRODUCTION

Recently, microfluidic devices have found important applications in microbiological sensors and micro-electro-mechanical systems. There are very comprehensive reviews on the fluid mechanics and various applications [1,2]. One way to transport fluids through microtubes in these miniaturized devices without mechanical moving parts is to utilize electro-osmosis (EO) driven by applied voltages [3,4]. Modeling EO flow involves coupling the underlying physics of mass transport, fluid flow, and electrostatics or electromagnetics. It is of essential importance to seek an understanding of the transport mechanisms by solving appropriate equations based on the physical laws describing the EO flow and the charge distributions.

In the literature, various theoretical and numerical studies have been conducted for EO flow in microchannels under different geometries and physical conditions. However, the EO flow system may be situated in a rotating environment, such as in centrifuges for flow control or mass separation. Duffy *et al.* [5] conducted experiments for investigating the use of centrifugal microfluidic systems for electrokinetic control of liquid flow in multiple enzymatic assays. It was suggested that such centrifugation may relieve the problem of Joule heating and complements EO as a means for pumping liquids in a range of wider channel sizes from 5 μm to $>$ 1 mm. Another good advantage of using a centrifuge is that the centrifugal pump can work when air is present along with a liquid in the microfluidic network, as the pump also works to dispel bubbles of gas. Despite these aspects of importance, analysis weighting the relative importance of transports by EO and rotating is still lacking. The aim of the present paper is to quantify the interactions of system rotation and EO by identifying the primary parameters that determine the flow rates and the relevant flow mechanisms.

Rotating flow is a classical subject. There are an abundant number of papers for viscous flow in a rotating environment. Reference [6] reported the effects of background rotation on fluid motions under various physical conditions. The typical interests include flow stability, secondary flow, transition to oscillatory or turbulent flow, as well as the effect of the resulting flow on the rate of heat transfer. In particular, a physical understanding of (secondary) transverse flow is important in any fluid problem. The secondary flow affects the transport of mass and energy, aside from generating vorticity for mixing. One type of secondary flow is from the flow in curved tubes; a secondary EO flow in a curved tube recently was reported in Refs. [7,8]. Analogously, the flow in a straight tube under system rotation also produces secondary flow, which is the primary concern of the present paper on the EO flow. On the other hand, rich literature on the effects of rotation can be found in the texts of geophysical fluid dynamics [9,10]. The rich background materials on rotating fluids provide a theoretical basis for analyzing the effects of rotation on EO flow. In a rotating system, aside from centrifugal pressure, the main effect of fluid flow inward is due to the Coriolis force, which alters the velocities and the fluid flux considerably. In a

*mechang@iam.ntu.edu.tw

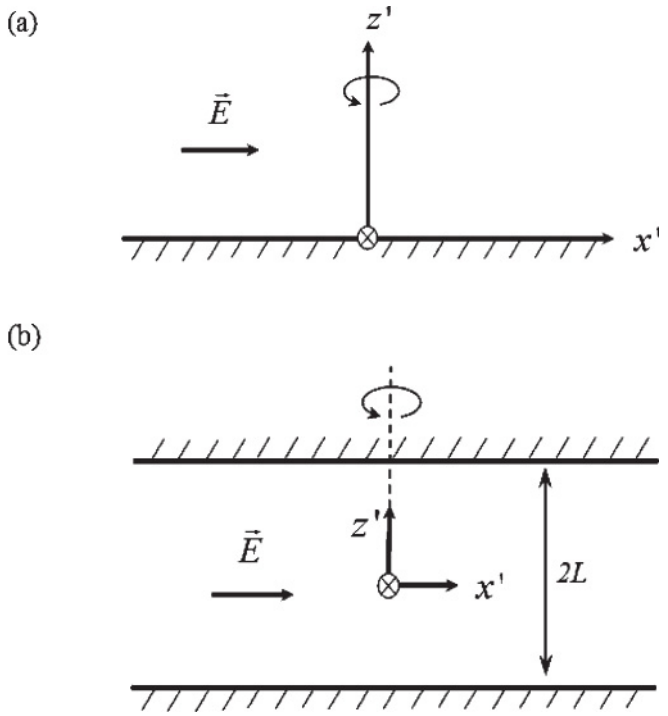

FIG. 1. (a) Schematic of rotating EO flow over an infinite plate. The electric field $\vec{E}$ is applied along the x' direction. The whole system (electrolyte plus the plate) is rotating about the z' axis vertical to the plate. The y' axis (denoted by $\otimes$) is pointing toward the inside of the plane. (b) Schematic of rotating EO flow between two infinite plates. The electric field $\vec{E}$ is applied along the axial x' direction. The whole system (electrolyte plus the plate) is rotating about the z' axis vertical to both plates. The y' axis (denoted by $\otimes$) is pointing toward the inside of the plane.

miniaturized microfluidic system, the flow Reynolds number is typically small. It is expected that steady-state flow is achieved by balancing the Coriolis force, pressure gradient, viscous force, and the body force due to the applied voltage. Due to the difficulty of the problem, we will consider two simple but fundamental cases shown in Fig. 1, namely, the effect of rotation on the EO flow over an infinite single plate and that in a channel formed between two parallel plates. As we will see, the two simple cases illustrate that system rotation not only produces lateral flow perpendicular to the applied field, but also has large effects on the throughflow. These simple but nontrivial problems enable the identification of relevant physical parameters due to rotation, which facilitate analyzing EO flow properties of fundamental interest in general rotating environments. Here, it is noted that, in this paper, if we need a physical quantity or a variable in both dimensional and nondimensional forms, the symbol with a prime denotes the dimensional one, and the same symbol without a prime is reserved for the nondimensional one.

II. THE INFINITE SINGLE PLATE

Consider a fluid over an infinite flat plate. Let (x',y',z') be Cartesian coordinates and z' be the normal to the plate. Due to symmetry, all variables are independent of the x',y' directions. Let ψ' be the electric potential due to the electric double layer (EDL). For low electric potentials compared to the thermal potential, the Debye-Hückel approximation for a symmetric electrolyte in dimensional form is given by [11]

$$\frac{d^2\psi'}{dz'^2} = \kappa^2\psi', \tag{1}$$

where κ is the Debye-Hückel parameter with its inverse $\lambda_D = 1/\kappa$ called the Debye length, defined by $\kappa^2 = 2z^2e^2n_0/\varepsilon k_BT$ where e is the electron charge, ε is the electric permittivity of the fluid, z is the valence, n_0 is the bulk electrolyte concentration, k_B is the Boltzmann constant, and T is the absolute temperature. The equation is subject to the boundary conditions: ζ potential $\psi' = \varsigma$ on the boundary (shear plane) and ψ' decaying to zero at infinity.

Notice that, in this problem, there is no natural length scale. Normalize all the lengths by $1/\kappa$, the EDL potential ψ' by ς, and drop the primes; then Eq. (1) with the boundary conditions becomes

$$\frac{d^2\psi}{dz^2} = \psi, \quad \psi(0) = 1, \quad \psi(\infty) = 0. \tag{2}$$

The solution to Eq. (2) is the well-known simple decaying $\psi = e^{-z}$.

In a system rotating with angular velocity $\vec{\Omega}$, the steady-state Navier-Stokes equations for constant density fluid in dimensional form is given by [12]

$$\rho\,(\vec{u}'\cdot\nabla'\vec{u}' + 2\vec{\Omega}\times\vec{u}') = \vec{f} - \nabla'P + \mu\,\nabla'^2\vec{u}', \tag{3}$$

where ρ is the fluid density, μ is the dynamic viscosity, $\vec{q}$ is the velocity vector, $\vec{f}$ is the body force, and $P = p - \rho|\vec{\Omega}\times\vec{r}'|^2/2$ with $\vec{r}' = (x',y',z')$ is the pressure, which includes that due to the centrifugal force. The system rotates in the z' direction $\vec{\Omega} = (0,0,\Omega)$, and the velocity is parallel to the plate $\vec{u}' = (u',v',0)$. There is no pressure gradient in the flow field except for the centrifugal force (incorporated in P). The body force for EO is

$$\vec{f} = (-\rho_eE,0,0) \quad \text{with} \quad \rho_e = -\varepsilon\frac{d^2\psi'}{dz'^2}, \tag{4}$$

where ρ_e is the charge density of the electrolyte and $-E$ is the constant electric field applied in the x' direction. In this case of an infinite plate, we may seek the solution $u' = u'(z)$, $v' = v'(z)$ and may simplify Eq. (3) with the use of Eq. (4). Note that the first term on the left hand side of Eq. (3) and the second term on the right hand side are simply zero. Equation (3) combined with Eq. (4) can be written explicitly in component form

$$-2\rho\,\Omega v' = \varepsilon E\frac{d^2\psi'}{dz'^2} + \mu\frac{d^2u'}{dz'^2}, \tag{5}$$

$$2\rho\,\Omega\,u' = \mu\frac{d^2v'}{dz'^2}. \tag{6}$$

Normalize all the lengths by $1/\kappa$, ψ' by ς, and the velocity by $\varepsilon E\varsigma/\mu$. Then, Eqs. (5) and (6) are recast in the dimensionless form

$$\frac{d^2u}{dz^2} + 2\omega\,v = -\psi = -e^{-z}, \tag{7}$$

$$\frac{d^2v}{dz^2} - 2\omega\,u = 0, \tag{8}$$

where we introduced the nondimensional frequency ω by defining $\omega = \eta^2 = \Omega/(\kappa^2\nu)$ with $\nu = \mu/\rho$. Equations (7) and (8) apparently look similar to the equations for the Ekman layer but differ both physically and mathematically. The equations for the Ekman layer in the geophysical flow represent a balance among the viscous, the Coriolis, and the pressure forces, while Eqs. (7) and (8) for EO in the rotating frame represent balance among the viscous, the Coriolis, and the electrostatic forces.

The parameter η is a measure of the thickness of the electric double layer relative to the depth of the Ekman layer. More precisely, we have $\eta = \lambda_D/L_K$ where we recall the Debye length $\lambda_D = 1/\kappa$ and define the Ekman depth $L_K = (\nu/\Omega)^{1/2}$. The typical value of η is small, varying from 10^{-4} to order 1, as the Ekman depth is on the order of 10 μm in a high-speed centrifuge pump, while λ_D ranges from 10 nm to 10 μm. For example, λ_D is about 100 nm and L_K is 32 μm, and thus, $\eta = 3.1 \times 10^{-3}$ if we take a $10^{-5}M$ KBr solution with the mass density of $\rho = 1$ g/cm^3, the viscosity of $\mu = 1$ cP (centipoise), and the speed of rotation Ω to be 90 000 rpm (Optima L-90K, Beckman Coulter, Inc.). Nevertheless, the present paper, as a theoretical study, takes a further step to explore η in a wide range from 0 to 10.

The boundary conditions for Eqs. (7) and (8) are that (u,υ) are zero on the nonslip plate and decay rapidly to zero at infinity. To solve for the velocities, we seek the solution by constructing the complex function $\chi = u + i\upsilon$ where $i = \sqrt{-1}$. This facilitates a solution of Eqs. (7) and (8), which are combined to give

$$\frac{d^2\chi}{dz^2} - 2\omega i\chi = -e^{-z}. \tag{9}$$

The solution is

$$\chi = \frac{1}{(1-2\omega i)}(e^{-\sqrt{2\omega i}z} - e^{-z}). \tag{10}$$

The axial EO velocity in the direction of the applied field (with $\omega = \eta^2$) is

$$u = \mathrm{Re}(\chi) = \frac{1}{1+4\omega^2}\{e^{-\sqrt{\omega}z}[\cos(\sqrt{\omega}z) + 2\omega\ \sin(\sqrt{\omega}z)] - e^{-z}\}, \tag{11}$$

and the transverse flow velocity is

$$\upsilon = \mathrm{Im}(\chi) = \frac{1}{1+4\omega^2}\{e^{-\sqrt{\omega}z}[2\omega\ \cos(\sqrt{\omega}z) - \sin(\sqrt{\omega}z)] - 2\omega\, e^{-z}\}. \tag{12}$$

Note the decay and the oscillatory nature in z. The solution of Eqs. (11) and (12) shows that the parameter $\eta = \sqrt{\omega}$ simultaneously is the decay rate of the homogeneous solution and the wave number of the spatial oscillation. At the limit $\omega = 0$ (no rotation), we have the axial $u = 1 - e^{-z}$ and the transverse υ, of simply, zero. In the outer region far away from the EDL, u uniformly becomes 1. The effect of $\omega = \eta^2$ is very significant in that the axial velocity u never approaches 1 while eventually decaying to 0 in the outer region as long as ω is nonzero, no matter how small it is. Also, when ω is nonzero, the axial EO flow u is always accompanied by a transverse component υ, which is comparable to u in magnitude.

Figure 2 shows analogs of Ekman spirals in the u-υ plane at different ω's for the EO flow. In the geophysical flow, the

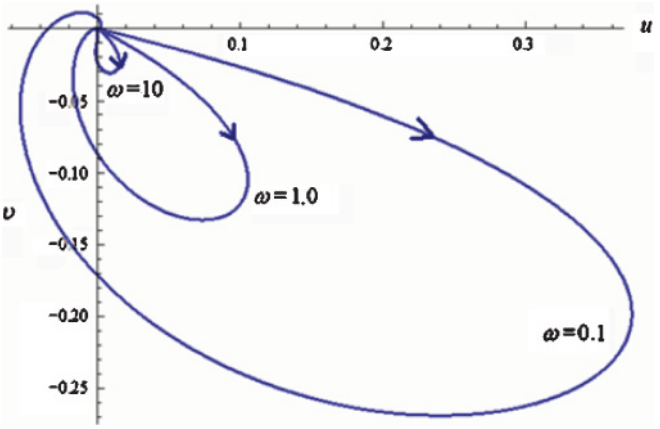

FIG. 2. (Color online) EO Ekman spirals on the u -υ plane for the single plate. For each ω, the spiral is a closed orbit, parametrized with respect to z, starting from the origin at $z = 0$ and clockwise approaching the origin as z tends to infinity.

Ekman spiral refers to a structure of currents or winds near a horizontal boundary in which the flow direction deviates from the external forcing and rotates as one moves away from the boundary. As a consequence, the volume transport associated with the Ekman spiral is to the right of the wind direction in the northern hemisphere. But the EO Ekman spirals are quite different, and the direction of the volume transport depends on ω. The EO spiral for each ω actually is a closed curve, the enclosed area of which becomes smaller with increasing ω. Each closed curve starts at the origin when $z = 0$. As z is increased (away from the plate), u moves in the positive x direction while υ (being negative) moves toward the right side of u (negative y direction). The initial direction is determined by taking the limit $(\upsilon/u) \to [2\omega - (1+2\omega)\sqrt{\omega}]/[1 + (2\omega - 1)\sqrt{\omega}]$ as $z \to 0$. After u reaches its maximum, the spiral turns around until $-\upsilon$ reaches its maximum. Then, both u and υ decrease in magnitude. Note that u eventually becomes negative (reflux) farther away from the boundary. In one of the plotted cases, υ may become positive. Finally, the circle spirals toward the origin.

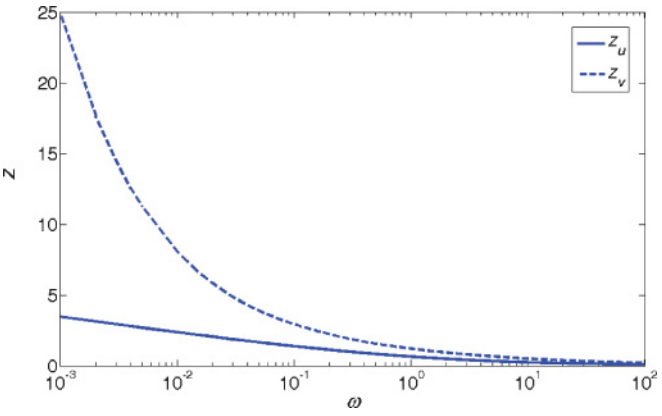

FIG. 3. (Color online) The location z_u of maximum $|u|$ (solid) and the location z_v of maximum $|\upsilon|$ (dashed) at different ω's for the EO flow over the single plate.

Figure 3 plots the pairs of values (z_u, z_v) where the velocities u and v attain their maxima for various ω. Notice that $2z_u$ and $2z_v$ may signify the respective ranges of the axial and transverse flows. Both ranges shrink as ω is increased. It is of interest to see that, in this case of a single infinite plate, the range of the transverse flow is two to five times wider than that of the axial flow. Also, this should have some implications on the flow rates q_x and q_y, which are obtained by integrating u and v in Eqs. (11) and (12) from $z = 0$ to infinity,

$$q_x = \frac{1}{1+4\omega^2}\left(\frac{1+2\omega}{2\sqrt{\omega}} - 1\right), \tag{13}$$

$$q_y = \frac{1}{1+\omega^2}\left(\frac{2\omega-1}{2\sqrt{\omega}} - 2\omega\right). \tag{14}$$

The results in Eqs. (13) and (14) immediately give the simple approximations,

$$(i)\ \ q_x \approx \frac{1}{2\sqrt{\omega}} \ \text{ for } \ \omega \ll 1; \quad q_x \approx \frac{1}{4\omega^{3/2}} \ \text{ for } \ \omega \gg 1;$$

$$(ii)\ \ q_y \approx -\frac{1}{2\sqrt{\omega}} \ \text{ for } \ \omega \ll 1; \quad q_y \approx -\frac{2}{\omega} \ \text{ for } \ \omega \gg 1.$$

It is not surprising at all that q_x is large when ω is small because q_x is infinity at $\omega = 0$. In contrast, q_y has the same magnitude as q_x even for very small ω as long as ω is nonzero, although q_y does vanish at $\omega = 0$ (when there only is an axial EO flow). But this is not unexpected because once the system is subject to rotation, the rotation starts to affect the flow equally well in both directions through the Coriolis force. The flow rates (like the velocity profiles) should indicate this effect when the flow reaches the steady state, although the passage from the starting flow to the steady state takes time. In the small ω limit, $q_y/q_x \approx -1$, the volume transport associated with the EO spiral makes a clockwise angle 45° with the applied electric field, while in the large ω limit, $q_y/q_x \approx -8\sqrt{\omega}$, which is nearly at right angles to the applied field. Figure 4 shows the details of flow directions by plotting $\beta = \tan^{-1}(q_y/q_x)$ versus ω, where β is the angle that the volume transport (q_x, q_y) associated with the EO Ekman spiral makes with the applied electric field. The EO volume transport deviates from the applied field by a clockwise 45° near $\omega = 0$ and effectively turns to be at right angles to the applied field as ω is increased.

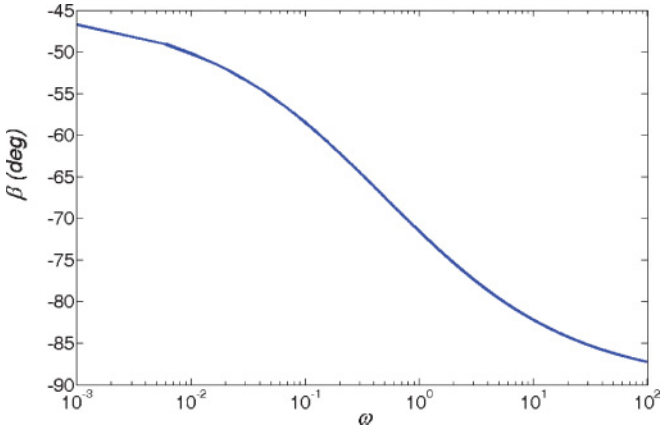

FIG. 4. (Color online) The angle $\beta = \tan^{-1}(q_y/q_x)$ that the volume transport associated with the EO Ekman spiral makes with the applied electric field versus ω. It is noted that β decreases monotonically with an increase in ω, being $-45°$ for very small ω and approaching $-90°$ in the limit of $\omega = \infty$.

III. THE CHANNEL BETWEEN TWO PARALLEL PLATES

A natural length scale exists for the channel. Let the channel height be $2L$ and normalize all lengths with respect to L. Let Cartesian axes (x, y, z) be placed at the midpoint such that $z = \pm 1$ represents the channel walls. The equation for the EDL potential is

$$\frac{d^2\psi}{dz^2} = K^2\psi, \tag{15}$$

where $K = \kappa L$ is the normalized Debye-Hückel parameter, and is called the dimensionless electrokinetic width, as a measure of the channel width (L) relative to the thickness of EDL $(1/\kappa)$. The solution to Eq. (15) with $\psi(\pm 1) = 1$ on the boundary is

$$\psi = \frac{\cosh(Kz)}{\cosh K}. \tag{16}$$

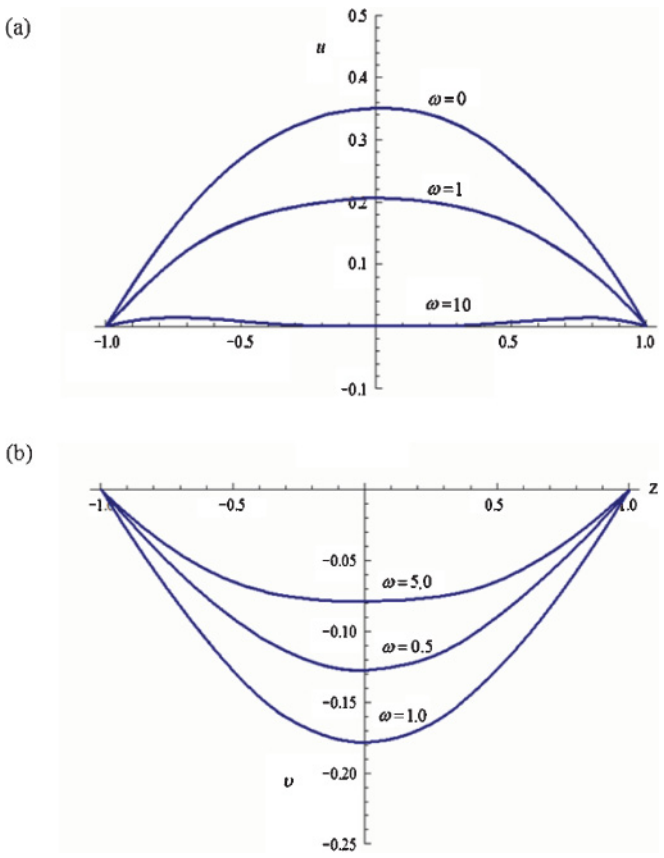

FIG. 5. (Color online) (a) The axial velocity u versus z with $K = 1$ for the channel between two parallel plates. From the top, $\omega = 0$, 1, 10; (b) the transverse v velocity in the $-y$ direction with $K = 1$ for the channel between two parallel plates. From the top, $\omega = 5$, 0.5, 1.

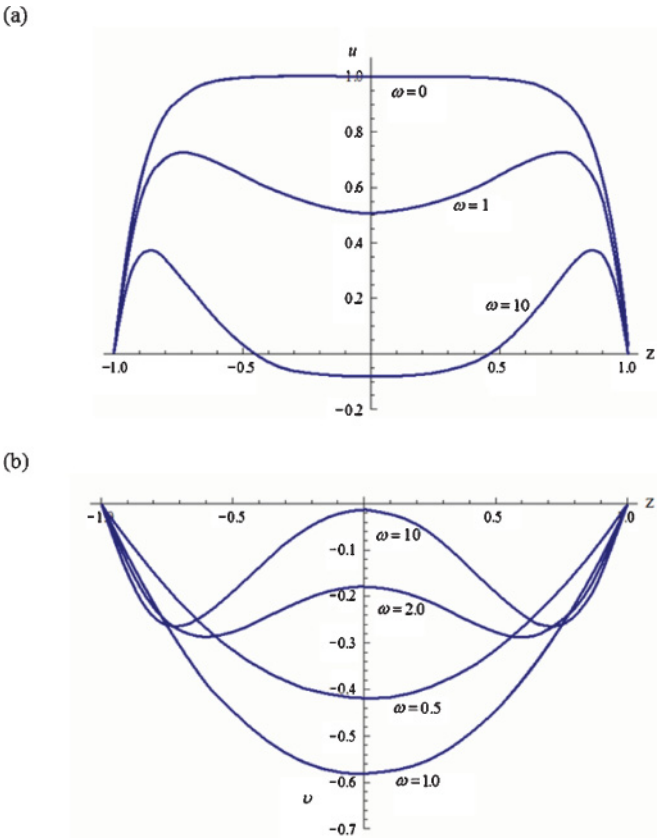

FIG. 6. (Color online) (a) The velocity u in the axial x direction with $K = 10$ for the channel between two parallel plates. From the top, $\omega = 0$, 1, 10; (b) the transverse υ velocity profile in the $-y$ direction versus z with $K = 10$ for the channel between two parallel plates. From the top at $z = 0$, ω =10, 2.0, 0.5, 1.0.

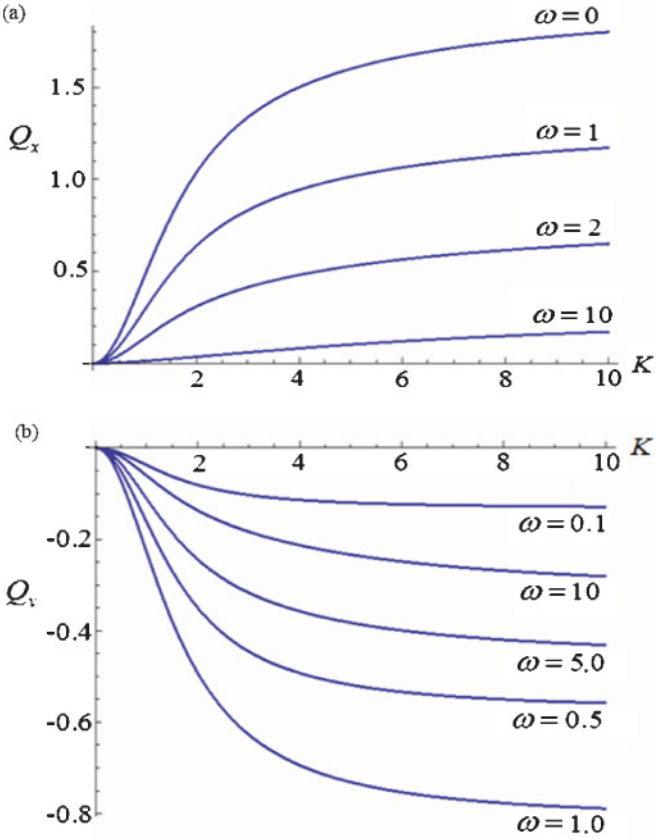

FIG. 7. (Color online) (a) The axial EO flow rate Q_x versus K for the channel between two parallel plates. From the top, $\omega = 0$, 1, 2, 10; (b) the transverse EO flow rate Q_y in the $-y$ direction versus K for the channel between two parallel plates. From the top, $\omega = 0.1$, 10, 5.0, 0.5, 1.0.

In the middle channel, the profile of ψ is a mild depression for small K and is a nearly zero flat valley for large K. Let $-E$ be the applied field in the x direction. After normalization, the governing fluid equations in a rotating system similarly can be derived

$$\frac{d^2u}{dz^2} + 2\omega\,\upsilon = -K^2\psi, \tag{17}$$

$$\frac{d^2\upsilon}{dz^2} - 2\omega\,u = 0, \tag{18}$$

where we introduced $\omega = \eta^2 = \Omega L^2/\upsilon$. Now, ω is no longer related to the thickness of the electric double layer; instead, it is a measure of fluid transport by rotation to that by the viscous effect. The parameter η can be written in several forms to see its various connections with others, $\eta = L/L_K = K/\kappa L_K = K\lambda_D/L_K$. Hence, η could vary in a wide range from 10^{-3} for a nanoscale channel of width $L = 10$ nm to the order 10 for a wider channel of width $L = 100$ μm, provided $L_K = 10$ μm.

Equations (17) and (18) can be solved similarly. Using $\chi = u + i\upsilon$ with ψ given in Eq. (16), we have the complex velocity χ that is even in z, and the no-slip zero velocities on the walls,

$$\chi = \frac{K^2}{(K^2 - 2\omega i)}\left[\frac{\cosh(\sqrt{2\omega i}\,z)}{\cosh(\sqrt{2\omega i})} - \frac{\cosh(Kz)}{\cosh K}\right]. \tag{19}$$

Define a complex volume flow rate per width normalized by $\varepsilon E\varsigma L/\mu$,

$$Q = Q_x + i\,Q_y = \int_{-1}^{1} \chi\,dz = \frac{2K^2}{(K^2 - 2\omega i)} \times\left[\frac{\tanh(\sqrt{2\omega i})}{\sqrt{2\omega i}} - \frac{\tanh K}{K}\right]. \tag{20}$$

The real part Q_x is the EO flow rate in the direction of the applied field, and the imaginary part Q_y is that normal to the applied field.

For some examples, consider the case $K = 1$. Note that, in this small K, the overlapped EDL potential in Eq. (16) has the minimum at the center of the channel ($z = 0$) and unity on the walls ($z = \pm 1$). Figures 5(a) and 5(b) show the distributions of the axial EO velocity u in the x direction and the induced lateral υ velocity in the $-y$ direction. It can be seen that, at this low electrokinetic width, the u velocity profile is almost parabolic if rotation is absent. The u profile remains nearly parabolic but is decreased greatly when there

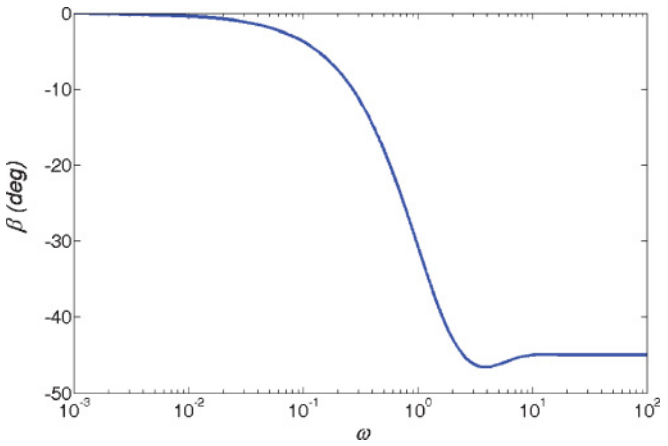

FIG. 8. (Color online) The angle $\beta = \tan^{-1}(Q_y/Q_x)$ made by the volume transport associated with rotating the EO flow between two plates with the applied electric field versus ω. It is seen that β is nearly 0° for small ω, varies most rapidly for ω between 0.1 and 2, attains the minimum -46.60° at $\omega = 3.855$, and approaches -45° in the limit of $\omega = \infty$.

is rotation (say, $\omega = 1$). The axial velocity u near the center region is even negative (reflux) for the high rotation at $\omega = 10$. In the same range of ω, the velocity profile of υ is basically parabolic, but the change in ω is not monotonic. The velocity υ has the maximum profile at $\omega = 1$. The υ velocity is zero for zero rotation and for infinite rotation rates. For the large $K = 10$, the EDLs on the two sides do not overlap, and the potential is restricted to boundary layers near the walls.

Figures 6(a) and 6(b) show the distributions of the axial EO velocity u in the x direction and the induced lateral υ velocity in the $-y$ direction. When there is no rotation, the u velocity has a flat velocity plateau at the interior. As ω is increased, the center velocity of u is reduced with the maximum of u shifting from the center toward the boundaries ($\omega = 1$). The center velocity even becomes negative for large rotations ($\omega = 10$). The induced υ velocity profiles exhibit a somewhat similar behavior in that the center velocity is reduced for high rotations. The υ velocity is parabolic for $\omega < 1$ and has the maximum parabolic profile at $\omega = 1$. Above $\omega = 1$, the velocity υ in the middle channel is much reduced as ω is further increased ($\omega > 1$).

Figures 7(a) and 7(b) plot the volume flow rates Q_x and Q_y given by Eq. (20) versus K for different speeds ω. When rotation is absent ($\omega = 0$), the axial EO flow rate increases from being proportional to K^2 for small K and approaches the constant Smoluchowsky limit of 2 as $K \to \infty$. When there is rotation $\omega > 0$, from Eq. (20), we find the limits of Q_x and Q_y for $K \to \infty$,

$$Q_x(\omega) = \frac{\sinh\sqrt{\omega}\cosh\sqrt{\omega} + \sin\sqrt{\omega}\cos\sqrt{\omega}}{\sqrt{\omega}(\cosh^2\sqrt{\omega} - \sin^2\sqrt{\omega})}, \quad (21)$$

$$Q_y(\omega) = \frac{\sin\sqrt{\omega}\cos\sqrt{\omega} - \sinh\sqrt{\omega}\cosh\sqrt{\omega}}{\sqrt{\omega}(\cosh^2\sqrt{\omega} - \sin^2\sqrt{\omega})}. \quad (22)$$

The results indicate that, in the limits of large $K \gg 1$, the (nondimensional) axial flow rate Q_x is 2 at $\omega = 0$, decreasing monotonically with an increase in ω, while the transverse flow rate Q_y is not a monotonic function of ω, being nearly zero for small ω and attaining its maximum at ω of order 1. Namely, in a range of small ω, the transverse flow Q_y is much smaller than Q_x. If we plot $\beta = \tan^{-1}(Q_y/Q_x)$ versus ω (Fig. 8), we see that the volume transport is almost at a zero angle to the applied field near $\omega = 0$, varies most rapidly for ω between 0.1 and 2, attains the minimum -46.60° at $\omega = 3.855$ and turns gradually to 45° (clockwise) to the applied field as ω is increased.

IV. CONCLUDING REMARKS

The paper presents a study of rotating EO flow over an infinite charged plate and for rotating EO flow in a microchannel formed by two charged parallel plates. The main findings are the occurrence of secondary (transverse) flow and its effects on the throughflow under various speeds of system rotation.

For the SP case, the axial velocity u is found to be oscillatory, decaying to zero at infinity. The degree of decay is determined by the smaller of the two rates: one due to the decaying EDL potential (particular solution) and η, the spatial oscillation frequency (homogeneous solution). The location of maximum velocity is shifted toward the plate with increasing ω. The plot in the u-υ plane shows interesting closed EO Ekman spiral orbits. The size of the closed orbit shrinks with an increase in ω. In the limits of small $\omega \ll 1$ (but not zero), both the axial and the transverse volume flow rates q_x and q_y are large in magnitude, scaled as $\pm 1/2\sqrt{\omega}$ respectively. In the limits of large $\omega \gg 1$, both flow rates q_x and q_y become small, scaled as $1/4\omega^{3/2}$ and $-2/\omega$, respectively. As $\omega \to \infty$, the entire fluid system nearly forms a rigid body rotation; there is neither axial nor transverse flow. The volume transport (q_x,q_y) associated with the Ekman spiral deviates from the applied field by a clockwise 45° near $\omega = 0$ and turns at right angles to the applied field as ω is increased.

For the TP case when the flow is confined to be between two plates, the flow behaviors are quite different. The transverse flow rates Q_y at all K are nearly zero (truly secondary) for both very small and very large ω and are observed to reach their maxima at ω of order 1. As ω is increased, the velocities u and υ become small in the middle channel with their maxima shifting toward the two side plates. Also, it is of interest to note that reflux in the axial velocity may even be observed to occur in the middle channel at large K by applying a higher rotation ω. No matter whether there is rotation or not, the axial Q_x increases with increasing the electrokinetic width K, and the reduction in Q_x by increasing ω is also more significant at larger K. As in the SP case, as $\omega \to \infty$, the entire fluid system nearly forms a rigid body rotation.

In conclusion, rotation reduces the EO flow rate in the direction of the applied field, equally for all K but with less significant secondary transverse flow in the TP case for small ω. Although the cases presented in this paper are less practical, as the channel has no lateral confinement, it is expected that, in cases with lateral walls, the EO flow in the axial direction also

will be altered effectively, accompanied by the occurrence of secondary flow across the channel. For example, in an annular channel, the lateral transverse flow may be used to mix the liquids as the EO flow proceeds in the direction of the applied field. Nevertheless, the details require further and separate investigation.

ACKNOWLEDGMENTS

The work is supported, in part, by the National Science Council of the Republic of China (Taiwan) under the Contracts No. NSC97-2221-E-002-223-MY3 and No. NSC 98-2628-M-002-004.

[1] T. M. Squires and S. R. Quake, Rev. Mod. Phys. **77**, 977 (2005).
[2] H. A. Stone, A. D. Stroock, and A. Ajdari, Annu. Rev. Fluid Mech. **36**, 381 (2004).
[3] H. Zhao and H. H. Bau, Phys. Rev. E **75**, 066217 (2007).
[4] K. A. Rose, B. Hoffman, D. Saintillan, E. S. G. Shaqfeh, and J. G. Santiago, Phys. Rev. E **79**, 011402 (2009).
[5] D. C. Duffy, H. L. Gillis, J. Lin, N. F. Sheppard, and G. J. Kellogg, Anal. Chem. **71**, 4669 (1999).
[6] E. J. Hopfinger and P. F. Linden, J. Fluid Mech. **211**, 417 (1990).
[7] W. J. Luo, Y. J. Pan, and R. J. Yang, J. Micromech. Microeng. **15**, 463 (2005).
[8] M.-S. Chun, Phys. Rev. E **83**, 036312 (2011).
[9] J. Pedlosky, *Geophysical Fluid Dynamics* (Springer-Verlag, New York, 1987).
[10] B. Cushman-Roisin, *Introduction to Geophysical Fluid Dynamics* (Prentice Hall, New York, 1994).
[11] C. C. Chang and C. Y. Wang, Phys. Fluids **21**, 042002 (2009).
[12] H. P. Greenspan, *Theory of Rotating Fluids* (Cambridge University Press, Cambridge, UK, 1968).